Phytopathologia Mediterranea
The international journal of the
Mediterranean Phytopathological Union

Firenze University Press
www.fupress.com/pm

Research Papers

Montmorillonite nanoclay triggers immunity responses in wheat against *Puccinia striiformis* f. sp. *tritici*, and suppresses uredospore germination

Younes M. RASHAD[1,*], Mohamed HAFEZ[2], Mohamed BOUROUAH[3], Ahmed M. ABD-ELGAWAD[4], Hany H.A. EL-SHARKAWY[5]

[1] *Plant Protection and Biomolecular Diagnosis Department, Arid Lands Cultivation Research Institute (ALCRI), City of Scientific Research and Technological Applications (SRTA-City), New Borg El-Arab City, 21934, Egypt*
[2] *Land and Water Technologies Department, Arid Lands Cultivation Research Institute (ALCRI), City of Scientific Research and Technological Applications (SRTA-City), New Borg El-Arab, 21934, Egypt*
[3] *Hahn-Schickard-Gesellschaft für angewandte Forschung e V., Wilhelm-Schickard-Straße 10, 78052 Villingen Schwenningen, Germany*
[4] *Plant Production Department, College of Food & Agriculture Sciences, King Saud University, P.O. Box 2460 Riyadh 11451, Saudi Arabia*
[5] *Mycology Research and Diseases Survey Department, Plant Pathology Research Institute, Agricultural Research Center, Giza, Egypt*
*Corresponding author. E-mail: younesrashad@yahoo.com

Summary. *Puccinia striiformis* f. sp. *tritici* causes the important disease, yellow rust of wheat (*Triticum aestivum*). Montmorillonite nanoclay (MNC) is naturally occurring and biodegradable. This study assessed *in vitro* anti-germination effects of MNC on *P. striiformis* uredospores. Application of MNC at 150 mg L^{-1} completely inhibited uredospore germination, and MNC at 100 mg L^{-1} reduced yellow rust severity in wheat plants by 89%. Expression of defense-related genes was increased after MNC treatment at 100 mg L^{-1}, by 5.23-fold for jasmonate and ethylene-responsive factor 3 (*JERF3*), 4.89-fold for chitinase class II (*CHI II*), and 2.37-fold for pathogenesis-related protein 1 (*PR1*). Applying MNC at 100 mg L^{-1} also activated the antioxidant enzymes POD to 62.1 unit min^{-1} g^{-1} fresh wt, PPO to 21.6 units min^{-1} g^{-1} fresh wt, and CAT to 36.6 units min^{-1} g^{-1} fresh wt. MNC also enhanced phenolic content in wheat leaves (to 1489.53 mg 100 g^{-1} f. wt), and reduced lipid oxidation levels (to 5.6 µmol MDA g^{-1} fresh wt). MNC at 100 mg L^{-1} also mitigated damaging effects of *P. striiformis* infections on host leaf cell ultrastructure, increased leaf photosynthetic pigments, and increased wheat plant growth. These results show that MNC has potential as a natural control agent for yellow rust of wheat, although field testing of MNC is necessary before this material can be recommended for wheat production.

Keywords. Nanoclay, host resistance, defense, *Triticum aestivum*, yellow rust.

OPEN ACCESS

Citation: Rashad, Y.M., Hafez, M., Bourouah, M., Abd-ElGawad, A.M., & El-Sharkawy, H.H.A. (2024). Montmorillonite nanoclay triggers immunity responses in wheat against *Puccinia striiformis* f. sp. *tritici*, and suppresses uredospore germination. *Phytopathologia Mediterranea* 63(2): 269-281. doi: 10.36253/phyto-15291

Accepted: August 5, 2024

Published: September 15, 2024

Data Availability Statement: All relevant data are within the paper and its Supporting Information files.

Competing Interests: The Author(s) declare(s) no conflict of interest.

Editor: Alessandra Lanubile, Università Cattolica del Sacro Cuore, Piacenza, Italy.

ORCID:
YMR: 0000-0002-7702-8023
MH: 0000-0001-9269-2128
MB: 0009-0001-3311-3816
AMA-E: 0000-0002-5903-6329
HHAE-S: 0000-0002-9386-6852

INTRODUCTION

Nanoclays are clay minerals consisting of particles in nanometer size ranges (1 to 100 nm). These minerals are classified as phyllosilicates, and are composed of stacked layers of aluminum and silicon oxides (Nazir *et al*., 2016). Nanoclays are known for their widespread presence in different environments, their high cation exchange capacity, affordability, and overall non-toxic nature. These properties allow them to form polymer nanocomposites which are carriers for active compounds and bioagents. These polymer nanocomposites have extensive applications in medicine, agriculture, and other technological applications, forming the nanoclay technology (Hafez *et al*., 2022).

Nanoclay research has focused on harnessing potential of materials in several fields (Merino *et al*., 2021). Agricultural uses of different nanoclay types, including montmorillonite, have been studied mainly for their antimicrobial activities (Yousef *et al*., 2023) and aflatoxin B1 detoxification potential in animal feeds (Soltan *et al*., 2022). Rashad *et al*. (2021a) reported effective spraying of silica nanoparticles (at 150 ppm) against downy mildew of grapevines, caused by *Plasmopara viticola*. A reduction (82%) in the disease severity and induction in the plant defense responses were recorded. Guilger-Casagrande *et al*., (2024) found that nanoparticles of iron oxide and titanium dioxide had high insecticidal potential on larvae of the crop pests *Helicoverpa armigera* and *Spodoptera frugiperda*, recording up to 76% mortality of these insects.

Montmorillonite is a clay mineral (smectite category), and consists of a layer of alumina enclosed between two layers of silica. Montmorillonite nanoclay (MNC) is widely used as a nanocomposite to form nano antimicrobials and pesticides against several plant diseases (Hossain *et al*., 2023). Oliveira-Pinto *et al*. (2022) reported effective potential of MNC alone or supplemented with *Satureja montana* essential oil, for control of bacterial spot in tomato, caused by *Xanthomonas euvesicatoria*. Antimicrobial, antioxidant, and defense triggering activities of MNC have been discussed as disease management strategies. Sundaresha *et al*. (2022) found that spraying potato plants with multigene-targeted dsRNA molecules carried on nanoclay particles reduced severity of late blight and inhibited growth and sporulation of *Phytophthora infestans*. In general, nanoparticles can be used to control different plant diseases, either as alone as protectants (Rashad et al., 2021a) or as carriers for fungicides or other antimicrobial substances (Worrall *et al*., 2018).

Wheat (*Triticum aestivum*) is the main staple diet for much of the world population. However, this crop is adversely affected by many fungal pathogens that are production threats. *Puccinia striiformis* Westend. f. sp. *tritici* Eriks, which causes stripe rust (yellow rust) of wheat, is a destructive pathogen that threatens wheat production (Chen *et al*., 2014). This obligate biotrophic basidiomycete fungus) is a heteroecious pathogen, infecting two alternate hosts (wheat and *Berberis* spp.) during its life cycle (Zhao *et al*., 2011). Under suitable climatic conditions, stripe rust infections can result in a severe wheat grain yield reduction of up to 100%. Fast growth, sporulation intensity, variability, and long-distance dispersal of air-borne *P. striiformis* uredospores are key properties that enable the fungus to cause severe yield damage (Chen *et al*., 2014).

Control of stripe rust has been widely studied using different agents to overcome development of *P. striiformis* race variability and rust resistance in wheat. El-Sharkawy *et al*. (2023a) achieved 88% reduction in yellow rust of wheat when sprayed with the endophyte *Epicoccum nigrum* Link (HE20). However, studies are lacking on impacts of MNC against wheat stripe rust. The present research was designed to investigate: 1) the inhibitory potential of MNC on *P. striiformis* uredospore germination; 2) disease control potential of MNC in greenhouse tests; 3) effects of MNC on transcriptomic profiles of defense genes in wheat plants; and 4) the effects of MNC applications on physiology, ultrastructure, and development of wheat plants.

MATERIALS AND METHODS

Fungal and plant materials

For the greenhouse experiment, infection of wheat plants was carried out using fresh uredospores of *P. striiformis* race 174E191. These spores were obtained from the Plant Pathology Research Institute, Agricultural Research Center (ARC), Giza, Egypt. To prepare inoculum, uredospores were suspended in sterilized water and adjusted to concentration of 10^4 spore mL^{-1} using a haemocytometer. Tween 80 (Sigma-Aldrich) was added at 0.3%, and gum Arabic (Stanton) was added to standardized uredospore suspensions at 35 g L^{-1}. The wheat cultivar Gemmaza 11 was used in experiments, and was obtained from ARC in Egypt.

Montmorillonite clay (MNC) preparation

The MNC used in this study was purchased from Egypt Bentonite and Derivatives Co., Alexandria, Egypt. To prepare MNC, montmorillonite clay parti-

cles were firstly modified with the organic surfactant CETAB (Sigma Aldrich) as described by Bujdáková *et al*. (2018). The modified MNC was ground using a planetary mill (PM 100, Verder Scientific) for 5 h at 300 rpm (reverse rotation), followed by 600 rpm (vial rotation) with nine zirconia grinding balls (35 mm diam.) and 12 (12 mm) (9:1 mass:mass) to obtain nano-scale particles (Soltan *et al*., 2022).

Characterization of MNC

To determine shape and size of MNC particles, dry nanoclay particles were put on a brass holder, coated with gold, and examined using a scanning electron microscope (SEM, JEOL-JSM-6360-LA), under vacuum and at accelerating voltage 20 Kv. To determine the element content of MNC, nanoclay particles were coated with gold and examined using an energy-dispersive X-ray spectroscope (EDX-Max), at a working voltage of 30 Kv. Functional groups in the MNC were identified using a Fourier-transform-infrared spectrophotometer (FTIR) (Shimadzu FTIR-8400S) equipped with a deuterated triglycine sulfate detector.

Assessment of the suppressive potential of MNC

Suppressive potential of MNC was tested against uredospore germination using the agar plate method *in vitro*. Petri plates (8 cm diam.) containing water agar (Merck) supplemented with MNC to obtain final concentrations of 10, 8, 6, 4, or 2% were each inoculated with 200 uredospores. Water agar plates without added MNC served as experimental controls. Three biological replicates and three technical replicates were applied for each treatment. The plates were incubated at 9°C for 1 d, and uredospore germination was assessed, and percentage of germination suppression was calculated.

Evaluation of MNC for wheat rust control

Plastic pots (20 cm diam.), each containing 10 kg sterile soil, were each planted with ten wheat seeds that had been previously surface sterilized by soaking in hypochlorite solution (0.05%) for 1.5 min, then in ethyl alcohol (75%) for 1.5 min. The pots were fertilized twice, first at seed sowing and then 7 weeks later. For each fertilization, nitrogen, (1 g per pot) phosphorus (1.5 g) and potassium (1 g) were applied. At 60 d after sowing, the resulting wheat plants were sprayed with MNC solution (at 100, 150, or 200 mg L^{-1} water) until run-off. A set of plants sprayed with Crwan fungicide (El-Helb Pest. and Chem., Egypt) at 3 mL L^{-1} served as positive controls. For inoculations, suspensions of *P. striiformis* uredospores were sprayed onto the plants (at booting growth stage) 3 d after the experimental treatments were applied. For negative controls, a set of plants were sprayed with water. Fifteen pots per treatment were used, and all pots were irrigated twice each week. All plants were arranged in a completely randomized experimental design in a greenhouse (20°C/17°C, 14 h light/10 h dark daily regime, and 75-90 % humidity). Treatments assessed were: untreated uninoculated (control; C), untreated plus *P. striiformis* inoculated (P), fungicide treated plus inoculated (F + P), MNC at 100 mg L^{-1} plus inoculated (N1 + P), MNC at 150 mg L^{-1} plus inoculated (N2 + P), or MNC at 200 mg L^{-1} plus inoculated (N3 + P).

Stripe severity was assessed in the plants at 14 d after inoculation (dai), according to the scale of Peterson *et al*. (1948). Average disease severity coefficients were calculated by multiplying severity percentages by values according to disease type: resistant = 0.2, moderately resistant = 0.4, moderately susceptible = 0.8, and susceptible = 1 (Johnston and Browder, 1966).

Impact of MNC on wheat gene expression

Wheat leaves (second upper leaf) from the assessed treatments were sampled at 3 d after inoculation (dai) (booting stage). Total RNA was extracted from sampled leaves using a RNA extraction kit (Qiagen), following the manufacturer's instructions. The reverse transcription mixture contained RNA (30 ng, 2.5 µL), 10× buffer solution (3 µL), oligo (dT) primer (8 pmol μL^{-1}, 5 µL), dNTPs (13 mM, 2.5 µL), RT enzyme (Biolabs, (0.4 µL), and sterile RNase-free water (7.6 µL). The reaction was carried out at 42°C for 1.5 h, then at 85°C for 10 min. cDNA was prepared using a thermocycler (Sure-Cycler 8800, Agilent Technologies). The quantitative real-time PCR (qPCR) contained cDNA (55 ng; 2.5 µL), SYBR Green Mix (13 µL, Bioloine), forward and reverse primers (10 pmol μL^{-1}, 1.5 µL for each), and sterile water (1.5 µL). Triplicate qPCR reactions (biological and technical) were carried out as follows: one cycle at 95°C for 3 min, 40 cycles, each of 95°C for 15 s, 56°C for 30 s, and 72°C for 30 s. β-actin was used as the reference gene. The primer sequences used are indicated in Table 1. The Rotor-Gene-6000-system (Qiagene) was used for the qPCR. The comparative CT method ($2^{-\Delta\Delta CT}$, Livak and Schmittgen, 2001) was used to calculate the gene expression, using triplicate samples (biological and technical).

Table 1. Primer sequences used in quantitative real-time PCR to study transcriptional expression of the defense-related genes jasmonate and ethylene-responsive factor 3 (*JERF3*), chitinase class II (*CHI II*), and Pathogenesis-related protein 1 (*PR1*) in wheat leaves after application of montmorillonite nanoclay at 100 mg L^{-1}.

Gene name	Abbreviation	Sequence (5'-3')
Jasmonate and ethylene-responsive factor 3	*JERF3*-F	GCCATTTGCCTTCTCTGCTTC
	JERF3-R	GCAGCAGCATCCTTGTCTGA
Chitinase class II	*CHI II*-F	GCGTTGTGGTTCTGGATGACA
	CHI II-R	CAGCGGCAGAATCAGCAACA
Pathogenesis-related protein 1	*PR1*-F	ACTTGGCATCCCGAGCACAA
	PR1-R	CTCGGACACCCACAATTGCA
β-actin	*β-actin-F*	GTGGGCCGCTCTAGGCACCAA
	β-actin-R	CTCTTTGATGTCACGCACGATTTC

Effects of MNC on the biochemical indicators in wheat leaves

At 3 dai, wheat leaves from each treatment (second upper leaf from each plant) were sampled for biochemical analyses. Total phenolic compounds were estimated as described by Malik and Singh (1980), using the Folin–Ciocalteu reagent. Peroxidase (POD) activity was determined as described by Maxwell and Bateman (1967), and polyphenol oxidase (PPO) was determined as described by Galeazzi *et al.* (1981). Catalase (CAT) activity was determined as described by Chance and Maehly (1955). Lipid peroxidation, expressed as malondialdehyde, was estimated at 14 dai in wheat leaves, as described by HongBo *et al.* (2005). The method of Harborne (1984) was used to measure photosynthetic pigments. Four samples were used for assessments of each treatment.

Transmission electron microscopy (TEM)

Wheat leaves were sampled from the different experimental treatments at 7 dai. The samples were cut into small segments (1 cm^2) and dehydrated using serial dilutions of ethyl alcohol (10 to 100%) for 10 min at each concentration). The samples were treated with propylene oxide for 15 min, and then put into gelatin capsules containing Araldite® for 1 h. The samples were then incubated at 65°C for 62 h. A Reichert ultramicrotome was used for the ultrathin sectioning. The obtained sections (thickness 70 to 90 nm) were stained by uranyl acetate (2%) then lead citrate (3%). Examination of the samples was carried out using a trans-mission electron microscope (JEM-1230, JEOL Ltd), as described by Hayat (2000).

Effects of MNC on the plant growth

From each treatment, ten plants were randomly selected at 30 dai (ripening stage), and were uprooted, washed with tap water, then measured for plant heights (cm), dry weights (g) of shoots and roots, and leaf areas (cm^2). Leaf areas were measured using ImageJ software, while plant heights were determined using a flexible graduated tape measure. Plant weights were measured after the plants had been sampled were oven-dried (80°C for 48 h).

Statistical analyses

Normality of raw data was assessed by Shapiro tests before analysis of variance. One-way analysis of variance was applied to raw data. The experimental design was completely randomized ($y_{ij} = \mu_i + \varepsilon_{ij}$). Comparisons of means were carried out using Tukey's HSD test ($P \leq 0.05$) with CoStat package version 6.4) (CoStat, 2005).

RESULTS

Characterization of MNC

The MNC used in this study was characterized using different techniques to elucidate its structure and physicochemical features. SEM observation showed glomerations of MNC particles with layered surfaces, showing that the material had normal form of montmorillonite clay (Figure 1).

Figure 2 shows the FTIR analysis of MNC. The FTIR spectrum revealed existence of interlayer –OH peaks at wavenumbers 3693 and 3626 cm^{-1}, which is characteristic for vibrations of OH in montmorillonite. Additionally, the absorption band at wavenumber of 1633 cm^{-1} is attributed to –OH bending in adsorbed H_2O, and the peak at wavenumber 1089 cm^{-1} is characteristic for Si–O–Si vibration (out-of-plane). Furthermore, the peak at wavenumber of 992 cm^{-1} is character-

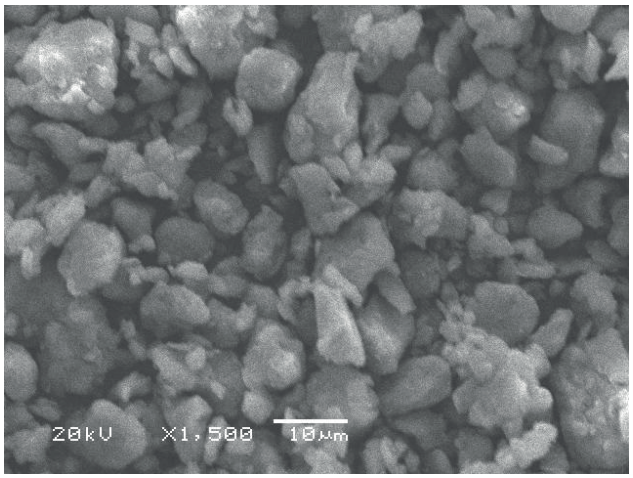

Figure 1. Scanning electron micrograph of the montmorillonite nanoclay used in this study. The cracked and rough particle surface morphology and agglomerations of particles with layered surfaces indicate normal form of the montmorillonite clay.

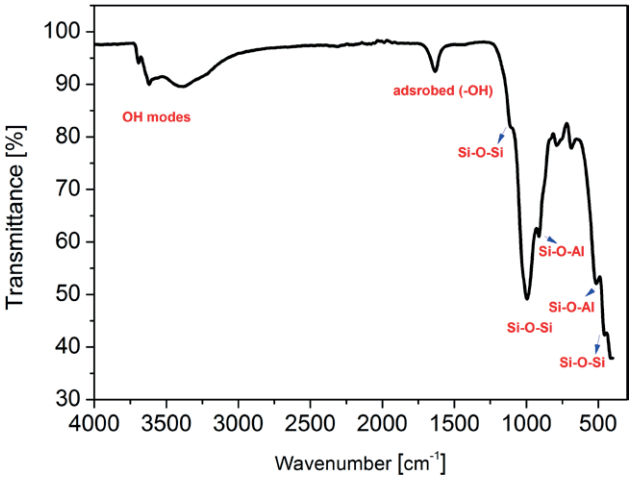

Figure 2. Fourier transformed infrared spectrum showing the functional groups in used montmorillonite nanoclay used in this study. The spectrum shows existence of the interlayer –OH peaks at 3693 and 3626 cm^{-1}. The absorption band at 1633 cm^{-1} is due to –OH bending. The peak at 1089 cm^{-1} is characteristic for the Si–O–Si vibration. The peak at 992 cm^{-1} is characteristic of in-plane Si–O–Si vibration. The area at 900 cm^{-1} is attributed to stretching of Si–O–Al. Vibration of Si–O–Al is also represented by the peak at 531 cm^{-1}, while that of Si–O–Si is represented by the peak at 472 cm^{-1}. The peak at 512 cm^{-1} is characteristic to vibration of Si–O–Al, while that at 462 cm^{-1} is characteristic to Si–O–Si vibration.

istic of in-plane Si–O–Si vibration, and the area at wavenumber 900 cm^{-1} is attributable to stretching of Si–O–Al. Bending vibration of Si–O–Al was represented by the peak at wavenumber of 531 cm^{-1}, while that of Si–O–Si was indicated by the peak at wavenumber of 472 cm^{-1}.

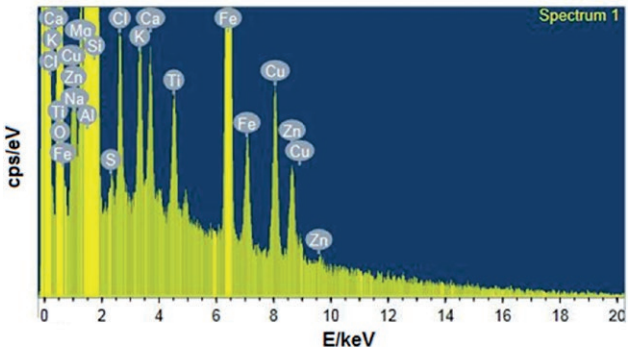

Figure 3. The energy-dispersive X-ray spectrum showing the elemental composition of the montmorillonite nanoclay used in this study. Element analysis showed presence of Na, Mg, Al, Si, K, and Ca. Other elements (S, Cl, Fe, Ti, Cu and Zn) were presented as traces.

Moreover, the peak at wavenumber of 512 cm^{-1} is characteristic of bending vibration of Si–O–Al, while the peak at wavenumber 462 cm^{-1} is characteristic to Si–O–Si bending vibration.

EDX analysis also showed that the major elements in the MNC were Na, Mg, Al, Si, K, and Ca, and other elements such as S, Cl, Fe, Ti, Cu and Zn were present as traces. The EDX spectrum is shown in Figure 3.

In vitro *assessment of suppressive potential of MNC*

Potential of MNC to suppress germination of *P. striiformis* uredospores was investigated *in vitro* (Table 2). Untreated uredospores exhibited normal germination (94.5 ± 2.44%). Treating uredospores with MNC at 150 or 200 mg L^{-1} completely suppressed germination, while treating them with MNC at 100 mg L^{-1} suppressed germination (89.2 ± 1.58%) compared to the untreated uredospores.

Assessments off disease severity

Table 3 shows effects of application of MNC on stripe rust at 14 dai. The pathogen caused 93.3% severity of stripe rust. Application of the fungicide reduced (by 96.5%) severity of the disease. Application of MNC at 100, 150, and 200 mg L^{-1} considerably reduced the disease severity leading, respectively, to reductions of 82.1, 82.1, and 78.6%, when compared with the control inoculated treatment (P). No differences ($P \leq 0.05$) were recorded between the three tested concentrations of MNC. Treatment (P) gave an average of 93.3% average coefficient of infection. The lowest average coefficient of infection (0.66%) was recorded from the F + P treatment

Table 2. Mean *in vitro* proportions of germination and inhibition of *Puccinia striiformis* f. sp. *tritici* uredospores treated with montmorillonite nanoclay (MNC) at different concentrations[a].

Treatment		Germination (%)	Inhibition (%)
Control		94.5 ± 2.4 a	0.0 c
MNC (mg L^{-1})	100	10.2 ± 1.3 b	89.2 ± 1.6 b
	150	0.0 c	100.0 a
	200	0.0 c	100.0 a
P-value ≤ 0.05			

[a]Means accompanied by different letters in each column are significantly different, according to Tukey's HSD test. Each value is the mean of three replicates ± SD. Anova significance values were as follows: germination (df = 5, F = 672.1); inhibition (df = 5, F = 1753.5).

Table 3. Mean stripe rust severity, reduction proportions and average coefficients of infection, after spraying wheat plants with montmorillonite nanoclay (MNC) at 14 days after inoculation with the pathogen[a].

Treatment	Disease severity (%)	Reduction (%)	Average coefficient infection (%)
C	0 c	0 c	0 d
P	93.3 ± 2.3 a	0 c	93.3 ± 2.3 a
F + P	3.3 ± 0.7 c	96.5 ± 3.1 a	0.66 ± 0.1 d
N1 + P	16.7 ± 1.1 b	82.1 ± 2.0 b	6.68 ± 1.1 c
N2 + P	16.5 ± 1.1 b	82.1 ± 1.8 b	6.68 ± 1.0 c
N3 + P	20.4 ± 1.2 b	78.6 ± 1.1 b	16.0 ± 1.7 b
P-value ≤ 0.05			

[a]Means accompanied by different etters in each column are significantly different according to Tukey's HSD test. Each value is the mean of ten replicates ± SD. Anova significance values were as follows: disease severity (df = 5, F = 640.2), reduction (df = 5, F = 1735.9), and average coefficient infection (df = 5, F = 1742.3). Non-sprayed and uninfected plants (C), non-sprayed and infected plants (P), plants sprayed with fungicide and inoculated (F + P), plants sprayed with MNC at 100 mg L^{-1} and inoculated (N1 + P), plants sprayed with MNC at 150 mg L^{-1} and inoculated (N2 + P), and plants sprayed with MNC at 200 mg L^{-1} and inoculated (N3 + P).

while application of MNC at 100, 150, or 200 mg L^{-1} led, respectively, to mean average coefficients of infection of 6.68, 6.68, and 16.0%

Effects of MNC on gene expression in wheat leaves

Transcriptional expression of *JERF3*, *CHI II*, and *PR1* in plant leaves following application of MNC at 100 mg L^{-1} is illustrated in Figure 4. Stripe rust infections did not affect the relative expression of *JERF3* and *CHI II*, while it led to a downregulation of *PR1*, compared to the control treatment (C). In contrast, spraying of the infected plants caused increased expression of the defensive genes *JERF3* (5.23-fold increase), *CHI II* (4.89-fold increase), and *PR1* (2.37-fold increase) when compared with the control plants.

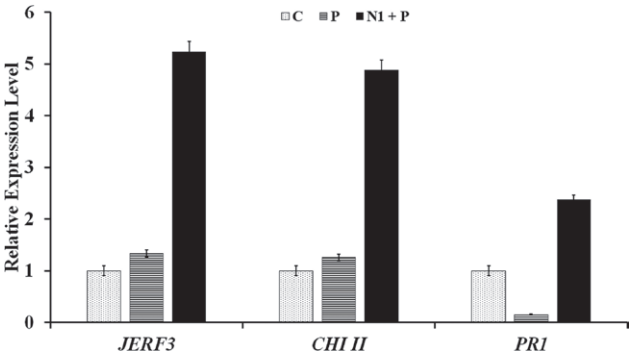

Figure 4. Mean relative transcriptional expression levels of the defense-related genes jasmonate-ethylene-responsive factor 3 (*JERF3*), chitinase II (*CHI II*), and the pathogenesis-related protein 1 (*PR1*) in wheat leaves in response to infections with *Puccinia striiformis* f. sp. *tritici* and application of the montmorillonite nanoclay (MNC) at 100 mg L^{-1}. The different coloured histograms indicate means for non-treated and uninfected plants (C), non-treated and infected plants (P), and plants sprayed with MNC at 100 mg L^{-1} and infected (N1 + P). Histograms for each gene which were superscripted with different letters are significantly different according to Tukey's HSD test ($P \leq 0.05$). For each treatment, three biological and three technical samples were used. Bars indicate the standard errors of the means.

Effects of MNC on plant defense biochemicals

Spraying the infected wheat plants with MNC affected production of several anti-oxidative stress enzymes, phenolic compounds, and lipid oxidation, at 3 dai (Table 4). Biochemical analyses showed that infections reduced activity of the enzymes POD, PPO, and CAT, and reduced phenolic contents, while infection increased lipid peroxidation, compared to the control treatment. Application of the fungicide activated POD and CAT, and enhanced the phenolic contents of the treated plants. Activity of PPO was not affected, and lipid oxidation was reduced by inoculation compared with treatment (P). MNC at most of the assessed concentrations activated POD, PPO, and CAT, (except for POD at MNC, 200 mg L^{-1}), and also increased wheat phenolic contents, while MNC reduced lipid oxidation, compared with treatment (P). The greatest enzymes activities and phenolic contents were recorded for the MNC treatments at 100 and 150 mg L^{-1}. The lowest mean lipid peroxida-

Table 4. Mean concentrations of enzymes, phenolic contents, and lipid peroxidation in wheat plants 3 d after inoculation with *Puccinia striiformis* f. sp. *tritici* and application of treatments with montmorillonite nanoclay (MNC) [a].

Treatment	Peroxidase (Unit $min^{-1}g^{-1}$ f. wt)	Polyphenol oxidase (Unit $min^{-1}g^{-1}$ f. wt)	Catalase (Unit $min^{-1}g^{-1}$ f. wt)	Phenolic content (mg.100 g^{-1} f. wt)	Lipid peroxidation (µmol MDA g^{-1} f. wt)
C	45.6 ± 3.6 b	8.0 ± 0.7 c	16.2 ± 2.3 c	862.6 ± 13.3 c	3.7 ± 0.3 e
P	26.5 ± 2.2 c	5.8 ± 0.6 d	12.6 ± 2.1 d	763.1 ± 10.2 d	13.2 ± 0.9 a
F + P	40.0 ± 2.5 b	6.9 ± 0.8 d	15.2 ± 1.5 c	824.3 ± 9.9 c	9.8 ± 0.9 b
N1 + P	62.1 ± 4.7 a	21.6 ± 1.4 a	36.6 ± 4.1 a	1489.5 ± 24.1 a	5.6 ± 1.0 d
N2 + P	60.1 ± 3.9 a	19.8 ± 1.1 ab	37.9 ± 3.9 a	1463.9 ± 22.4 a	7.2 ± 0.4 c
N3 + P	49.1 ± 1.5 b	18.2 ± 1.8 b	28.7 ± 3.8 b	1232.5 ± 21.8 b	9.6 ± 1.0 b
P-value ≤ 0.05					

[a]Means accompanied by different sletters in each column are significantly different according to Tukey's HSD test. Each value is the mean of ten replicates ± SD. Anova significance values were as follows: peroxidase (df = 5, F = 10.5), polyphenol oxidase (df = 5, F = 165.7), catalase (df = 5, F = 40), phenolic content (df = 5, F = 31.9), and lipid peroxidation (df = 5, F = 59.6). The treatments were: non-sprayed and uninoculated (C); non-sprayed and inoculated (P); sprayed with fungicide and inoculated (F + P); sprayed with MNC at 100 mg L^{-1} and inoculated (N1 + P); sprayed with MNC at 150 mg L^{-1} and inoculated (N2 + P); or sprayed with MNC at 200 mg L^{-1} and inoculated (N3 + P).

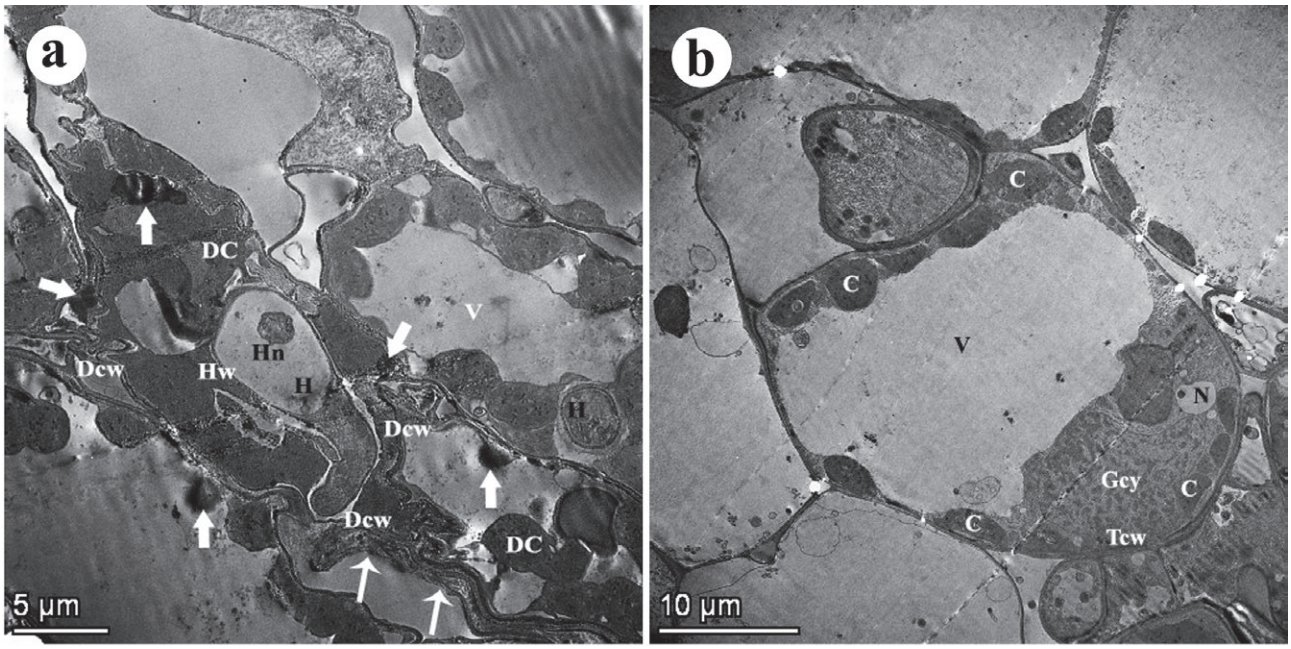

Figure 5. Transmission electron micrographs showing the cellular ultrastructure of wheat leaves which were infected with stripe rust and treated or not treated with montmorillonite nanoclay at 100 mg L^{-1} 7 d after the inoculation with the pathogen. a) an untreated inoculated leaf, and b) an infected leaf which was sprayed with montmorillonite nanoclay. H, haustoria; Hw, haustorium wall; Hn, haustorium nucleus; Dcw, decomposed cell wall; DC, degenerated chloroplast; V, vacuole; Tcw, thick cell wall; N, nucleus; C, chloroplast; Gcy,: granulated cytoplasm. Narrow arrows indicate intercellular fungal mycelium, while the broad arrows indicate electron dense bodies.

tion level (5.60 µmol MDA g^{-1} fresh weight) in the infected plants was recorded from MNC at 100 mg L^{-1}.

TEM observations

Effects of MNC (100 mg L^{-1}) application on ultrastructure of infected wheat cells are illustrated in Figure 5. Transmission electron micrographs showed that untreated inoculated leaves leaf contained large haustoria penetrating the mesophyll cells and growing between them. Host stress effects were also observed in the infected cells, including disorganization of the cells, degeneration of many chloroplasts, presence of electron dense bodies, and decomposition of some cell walls (Fig-

ure 5a). In contrast, tissue of the infected plant which had been treated with MNC did not show these disruptions. Cells from this tissue had normal organization and were enclosed by thick walls surrounding normal chloroplasts, and had large vacuoles, granulated cytoplasm, and normal nuclei (Figure 5b).

Effects of MNC on wheat photosynthetic pigments

Spraying MNC affected photosynthetic pigments in the infected wheat leaves at 14 dai (Table 5). Treatment (P) reduced chlorophyll *a* and *b* contents, and carotenoids, compared with treatment (C). Treatment (F + P) led to increases in all assessed pigments, compared with treatment (P). Application of MNC at all concentrations also increased contents of chlorophyll *a* and *b*, and carotenoids content, compared with treatment (P). The greatest amounts of total pigments were in the infected wheat sprayed with MNC at 100 or 150 mg L^{-1}, with both treatments resulting in means of 4.62 mg MNC g^{-1} fresh weight.

Effects of spraying MNC on plant growth

Treatment (P) (treatment of wheat plants with MNC) reduced all the assessed plant growth parameters, compared to treatment (C) (Table 6). Application of the fungicide enhanced all these growth parameters, compared to treatment (P), while spraying the infected wheat by MNC at 100, 150, or 200 mg L^{-1} increased all the

Table 5. Mean photosynthetic pigment contents in wheat leaves 14 d after inoculation with *Puccinia striiformis* f. sp. *tritici* and application of treatments with montmorillonite nanoclay (MNC) [a].

Treatment	Chlorophyll *a* (mg g^{-1} fresh weight)	Chlorophyll *b* (mg g^{-1} fresh weight)	Carotenoids (mg g^{-1} fresh weight)	Total pigments (mg g^{-1} fresh weight)
C	2.3 ± 0.2 b	1.0 ± 0.2 b	0.3 ± 0.06 c	3.5 ± 0.4 c
P	1.4 ± 0.2 d	0.8 ± 0.1 c	0.1 ± 0.05 d	2.3 ± 0.5 d
F + P	1.9 ± 0.1 c	1.0 ± 0.1 b	0.3 ± 0.02 b	3.1 ± 0.2 c
N1 + P	2.9 ± 0.4 a	1.4 ± 0.2 a	0.3 ± 0.04 b	4.6 ± 0.6 a
N2 + P	2.9 ± 0.4 a	1.3 ± 0.1 a	0.4 ± 0.08 a	4.6 ± 0.6 a
N3 + P	2.8 ± 0.2 ab	1.0 ± 0.2 b	0.5 ± 0.05 a	4.2 ± 0.5 b
P-value ≤ 0.05				

[a] Means accompanied by different letters in each column are significantly different, according to Tukey's HSD test. Each value is the mean of ten replicates ± SD. Anova significance values were: Chlorophyll *a* (df = 5, F = 14.9), Chlorophyll *b* (df = 5, F = 1.6), caroteniods (df = 5, F = 3.2), and total pigments (df = 5, F = 13.2). Treatments applied were: non-sprayed and uninoculated (C), non-sprayed and inoculated (P), sprayed with the fungicide and infoculatted (F + P), sprayed with MNC at 100 mg L^{-1} and inoculated (N1 + P), sprayed with MNC at 150 mg L^{-1} and inoculated (N2 + P), or sprayed with MNC at 200 mg L^{-1} and infected (N3 + P).

Table 6. Mean wheat plant parameters 30 d after inoculation with *Puccinia striiformis* f. sp. *tritici* and application of treatments with fungicide or montmorillonite nanoclay (MNC) [a].

Treatment	Plant height (cm)	Shoot dry weight (g)	Root dry weight (g)	Leaf area (cm^2)
C	56.4 ± 1.6 b	2.1 ± 0.4 bc	0.4 ± 0.01 c	18.3 ± 0.9 b
P	45.1 ± 1.3 c	1.2 ± 0.2 d	0.2 ± 0.04 e	11.1 ± 1.1 c
F + P	60.0 ± 3.6 ab	2.1 ± 0.3 c	0.3 ± 0.01 c	18.0 ± 1.1 b
N1 + P	51.1 ± 4.0 b	2.3 ± 0.3 b	0.5 ± 0.07 a	35.6 ± 4.5 a
N2 + P	69.0 ± 3.1 a	3.2 ± 0.7 a	0.5 ± 0.08 b	32.2 ± 4.1 a
N3 + P	53.3 ± 2.6 b	2.2 ± 0.6 b	0.3 ± 0.07 d	18.2 ± 1.2 b

[a]Means accompanied by different letters in each column are significantly different, according to Tukey's HSD test ($P \leq 0.05$). Each value represents the mean of ten replicates ± SD. Anova significance values were as follows: mean plant height (df = 5, F = 7.2); mean shoot dry weight (df = 5, F = 7.8); mean root dry weight (df = 5, F = 75.5);,mean leaf area (df = 5, F = 13).Non-sprayed and non-inoculated leaves (C); non-sprayed and inoculated leaves (P); leaves sprayed with fungicide and inoculated (F + P); leaves sprayed with MNC at 100 mg L^{-1} and inoculated (N1 + P); leaves sprayed with MNC at 150 mg L^{-1} and inoculated (N2 + P); leave sprayed with MNC at 200 mg L^{-1} and inoculated (N3 + P).

growth parameters. However, MNC at 150 mg L^{-1} gave the greatest increases in plant height, shoot dry weight and leaf area. Spraying *P. striiformis* infected plants with MNC at 150 mg L^{-1} usually improved the plant growth, and more so than the fungicide.

DISCUSSION

Several previous studies have focused on potential solutions for control of stripe rust in wheat, due to the importance of this disease which can cause up to complete yield losses in disease-conducive climatic conditions (El-Sharkawy *et al*., 2023 a and b). In the present study, the wheat stripe rust control potential of MNC was evaluated. Direct suppressive effects of MNC on uredospore germination was demonstrated *in vitro*, where applications of MNC at 150 or 200 mg L^{-1} completely suppressed germination, while MNC at 100 mg L^{-1} led to a strong germination inhibition (89.2 %). This anti-germination activity is consistent with the results of Iconaru *et al.* (2019), who reported antifungal potential of montmorillonite against growth of *Candida albicans*. This inhibitory potential was attributed to silicon and aluminum ions released from montmorillonite clay. However, due to nano size of the MNC particles assessed in this study, their contents of metal ions were greater than that in the micro sized particles of montmorillonite layer which led to increased antifungal activity.

Inhibitory potential of aluminum ions has been previously reported, and is causes imbalance of cellular ionic contents and inhibits messenger calmodulin protein (Kolaei *et al*., 2013). Reductions in spore germination caused by silicon ions were attributed to disruption of fungal spore plasma membranes, leading to leakage of cell contents (Liu *et al*., 2010). This may have been the cause of reductions in uredospore germination after MNC treatments observed in the present study. Uredospores germinate rapidly (within 3 h) before stomatal penetration, so suppression of germination is likely to control *P. striiformis tritici* by reducing inoculum loads. Direct inhibitory effects of MNC on uredospores played an important role in controlling rust in wheat plants.

Data obtained in the present study showed that spraying MNC at 100 mg L^{-1} gave greater than 80% reductions in stripe rust, compared to the untreated-inoculated control treatment [treatment (P)]. To investigate the mechanisms of disease control caused by MNC, expression profiles of *JERF3*, *CHI II*, and *PR1* were assessed in infected wheat leaves which were treated with MNC at 100 mg L^{-1}. Results showed that application of MNC at 100 mg L^{-1} gave overexpression of these genes. The response factor *JERF3* activates defense-related and stress-responsive genes in plants (Zhang *et al*., 2010). Rashad *et al.* (2021b) found that banana plants exhibiting upregulation of *JERF3* had increased tolerance to biotic and abiotic stresses. These plants also overexpressed multiple stress-responsive genes. *CHI II* is a defensive gene encoding for chitinase, and activates hydrolysis of chitin. This compound is a major component of fungal cell walls, and chitinase degrades glycoside bonds (Poria *et al*., 2021). Production of chitinase has potential for protection of wheat plants against invasion by *P. striiformis*, by degrading cell walls of penetrating haustoria and impairing their function. *PR1* encodes for the pathogenesis-related protein 1, a stress responsive protein which accumulates against various stresses, and is used as a marker for triggered plant defense, particularly within the salicylic acid pathway (Li *et al*., 2021). This protein has multiple functions, including signal transduction, cell wall rigidification, and fungitoxic potential. Farrakh *et al.* (2018) recorded overexpression of *PR1* in *P. striiformis*-infected wheat. They found that the *PR1* gene affected race-specific immunity regulated by *Yr* genes. In contrast, results obtained in the present study showed that stripe rust did not affect relative expression of *JERF3* and *CHI II*, while it led to downregulation of *PR1*, compared to control plants. This result is similar to those of Rashad *et al.* (2024), who reported downregulation of six of 13 polyphenol genes in response to stripe rust. Breakdowns of immunity to *P. striiformis* have been reported in different wheat varieties (Gultyaeva *et al*., 2022).

Spraying MNC on the infected wheat plants activated the antioxidant enzymes POD, PPO, and CAT, and increased phenolic contents, while this material also lowered lipid oxidation levels. Reactive oxygen species have important roles in virulence of *P. striiformis*. This pathogen produces superoxide radicals, hydrogen peroxide, and hydroxyl radicals through infection processes, which are important for uredospore germination and fungal development in plants (Wang *et al*., 2020). Therefore, induction by MNC of these antioxidant enzymes mitigate infection impacts on plant cells, and reduce pathogen virulence. This result was supported by the TEM observations (Figure 5b), which showed mitigation of stress in infected plants that were sprayed with MNC.

POD and CAT enzymes catalyze oxidative reactions by breaking down hydrogen peroxide (Vidossich *et al*., 2012). The enzyme PPO catalyzes oxidation of phenols to quinones, that are more toxic to *P. striiformis* than phenols (Zhang, 2023). Phenolic compounds such as phenolic acids, flavonoids, and flavonols have defense functions in plants through multiple antifungal effects (Rashad *et*

al., 2020a), and are used as markers for induced resistance in plants (Rashad *et al*., 2018). Rashad *et al.* (2020b) reported that induced resistance against garlic white rot (caused by *Sclerotium cepivorum*) , was accompanied with increases in total phenols. In addition, lignin deposition is an important host defense mechanism for restricting penetration of *P. striiformis* into plant cells and limiting nutrient intake by haustoria (El-Sharkawy *et al*., 2023b). These observations demonstrated the induction of immunity responses by MNC applications to in the infected wheat plants.

Spraying MNC onto wheat plants increased all the evaluated growth parameters, while high rate of MNC reduced some parameters. Most nanoparticles have cytotoxic and genotoxic effects at high concentrations, which may negatively affect plant physiological processes (Rashad *et al*., 2021a). Reduction of infection due to application of MNC mitigated effects of *P. striiformis* on plant growth. Spraying with MNC enhanced contents of chlorophyll *a* and *b*, and carotenoids. These photosynthetic pigments are essential for plant growth, and they are indicators of host physiological status under environmental stresses (Al-Askar *et al*., 2014; Esteban *et al*., 2015). Rust diseases destroy chloroplast ultrastructure in wheat leaves, as was observed from the TEM observations in the present study (Figure 5a). This leads to decreased chlorophyll *a* and *b*, and carotenoids, and reduced photosynthetic activity. Furthermore, thylakoid membranes and proteins are also destroyed (Chen *et al*., 2015). El-Sharkawy *et al.* (2023a) found that wheat rust adversely affects photosynthetic contents in host leaves. Analysis of MNC in the present study indicated that it contained plant nutrient including Mg, Na, S, K, Ca, Fe, Cu, and Zn. Mg ions are the central components of chlorophyll molecules, and activate plant enzyme system in plants and are involved in protein synthesis. The other elements have growth-enhancing effect on plants, and are also involved in cell wall rigidity, enzymes activation, protein synthesis, and other important plant metabolic processes (Ishfaq *et al*., 2022).

CONCLUSIONS

This study has demonstrated the suppressive effects of MNC on *P. striiformis tritici* uredospore germination, and ability of this nanoclay to induce wheat defensive responses against stripe rust. The study showed that overexpression of *JERF3*, *CHI II*, and *PR1* followed MNC treatments. Additionally, spraying MNC activated POD, PPO, and CAT enzymes, increased plant phenolic contents, and reduced lipid oxidation in wheat leaves. MNC applications also reduced the damaging effects of the pathogen on the leaf cell ultrastructure, and enhanced contents of photosynthetic pigments and plant growth. MNC is biodegradable and naturally occurring, so is environmentally "friendly". Based on these results, MNC has promise as a natural control agent against yellow rust of wheat. However, further evaluation of MNC under field conditions is necessary before practical disease control can be recommended.

ACKNOWLEDGMENTS

The authors are grateful to Prof. Abu Bakr A. Amine of SRTA-City for his assistance with physical characterization of MNC. They also acknowledge funding support for the reported research from The Researchers Supporting Project number RSPD2024R676, at King Saud University, Riyadh, Saudi Arabia.

AUTHOR CONTRIBUTIONS

Y.M. Rashad contributed to the research concept, formal analyses, investigation, and manuscript preparation, writing, and revision. A.M. Abd-ElGawad contributed to the resources and revision of the manuscript. M. Hafez and M. Bourouah contributed to data analyses and revision of the manuscript. H.E. El-Sharkawy contributed to investigation, and data curation. All the authors have read and agreed to publication of the final version of the manuscript.

LITERATURE CITED

Al-Askar A.A., Abdulkhair W.M., Rashad Y.M., Hafez E.E., Ghoneem K.M., Baka Z.A., 2014. Streptomyces griseorubens E44G: A Potent Antagonist Isolated from Soil in Saudi Arabia. *Journal of Pure and Applied Microbiology* 8: 221–230.

Bujdáková H., Bujdáková V., Májeková-Koščová H., Gaálová B., Bizovská V., … Bujdák J., 2018. Antimicrobial activity of organoclays based on quaternary alkylammonium and alkylphosphonium surfactants and montmorillonite. *Applied Clay Science* 158: 21–28. https://doi.org/10.1016/j.clay.2018.03.010.

Chance B., Maehly A.C.B.T.-M. in E., 1955. Assay of catalases and peroxidases: In: *Methods in Enzymology*, Academic Press, 764–775.

Chen W., Wellings C., Chen X., Kang Z., Liu T., 2014. Wheat stripe (yellow) rust caused by *Puccinia strii-*

formis f. sp. *tritici*. *Molecular Plant Pathology* 15: 433–446. https://doi.org/10.1111/mpp.12116.

Chen Y.E., Cui J.M., Su Y.Q., Yuan S., Yuan M., Zhang H.Y., 2015. Influence of stripe rust infection on the photosynthetic characteristics and antioxidant system of susceptible and resistant wheat cultivars at the adult plant stage. *Frontiers in Plant Science* 6: 779. https://doi.org/10.3389/fpls.2015.00779.

CoStat, 2005. *Cohort Software*. 798 Lighthouse Ave., PMB 320 Monterey, USA.

El-Sharkawy H.H.A., Rashad Y.M., Elazab N.T., 2023a. Biocontrol potential of the endophytic *Epicoccum nigrum* HE20 against stripe rust of wheat. *Pesticide Biochemistry and Physiology* 194: 105517. https://doi.org/10.1016/j.pestbp.2023.105517.

El-Sharkawy H.H.A., Rashad Y.M., Elazab N.T., 2023b. Induction of multiple defense responses in wheat plants against stripe rust using mycorrhizal fungi and Streptomyces viridosporus HH1. *BioControl* 68(5): 525–535. https://doi.org/10.1007/s10526-023-10207-4.

Esteban R., Barrutia O., Artetxe U., Fernández-Marín B., Hernández A., García-Plazaola J.I., 2015. Internal and external factors affecting photosynthetic pigment composition in plants: A meta-analytical approach. *New Phytologist* 206: 268–280. https://doi.org/10.1111/nph.13186.

Farrakh S., Wang M., Chen X., 2018. Pathogenesis-related protein genes involved in race-specific all-stage resistance and non-race specific high-temperature adult-plant resistance to *Puccinia striiformis* f. sp. *tritici* in wheat. *Journal of Integrative Agriculture* 17: 2478–2491. https://doi.org/10.1016/S2095-3119(17)61853-7.

Galeazzi M.A.M., Sgarbieri V.C., Constantinides S.M., 1981. Isolation, purification and physicochemical characterization of polyphenol oxidase (PPO) from a dwarf variety of banana (*Musa cavendishii*, L). *Journal of Food Science* 46: 150–155. https://doi.org/10.1111/j.1365-2621.1981.tb14551.x.

Guilger-Casagrande M., Migliorini B.B., Germano-Costa T., Bilesky-José N., Harada L.K., … Lima R., 2024. *Beauveria bassiana* biogenic nanoparticles for the control of Noctuidae pests. *Pest Management Science* 80: 1325–1337. https://doi.org/10.1002/ps.7863.

Gultyaeva E., Shaydayuk E., Kosman E., 2022. Virulence Diversity of Puccinia striiformis f. sp. Tritici in Common Wheat in Russian Regions in 2019–2021. *Agriculture (Switzerland)*.

Hafez M., Ahmed A.A., Mohamed A.E., Rashad MM., 2022. Influence of environmental-friendly bio-organic ameliorants on abiotic stress to sustainable agriculture in arid regions: A long term greenhouse study in northwestern Egypt. *Journal of King Saud University - Science* 34(6): 102212.

Harborne J.B., 1984. *Phytochemical Methods: A guide to Modern Techniques of Plant Analysis*. London: Chapman and Hall.

Hayat M.A., 2000. *Principles and Techniques of Electron Microscopy*. Biological Applications, 4th edition. Cambridge University Press, Cambridge, United Kingdom.

HongBo S., ZongSuo L., MingAn S., 2005. Changes of anti-oxidative enzymes and MDA content under soil water deficits among 10 wheat (*Triticum aestivum* L.) genotypes at maturation stage. *Colloids and Surfaces. B, Biointerfaces*, Netherlands 45: 7–13. https://doi.org/10.1016/j.colsurfb.2005.06.016.

Hossain S.I., Kukushkina E.A., Izzi M., Sportelli M.C., Picca R.A., … Cioffi N., 2023. A Review on Montmorillonite-Based Nanoantimicrobials: State of the Art. *Nanomaterials* 13(5): 848

Iconaru S.L., Groza A., Stan G.E., Predoi D., Gaiaschi S., … Chapon P., 2019. Preparations of Silver/Montmorillonite Biocomposite Multilayers and Their Antifungal Activity. *Coatings* 9: 817.

Ishfaq M., Wang Y., Yan M., Wang Z., Wu L., … Li X., 2022. Physiological Essence of Magnesium in Plants and Its Widespread Deficiency in the Farming System of China. *Frontiers in Plant Science* 13: 802274.

Johnston C.O., Browder L.E., 1966. Seventh revision of the international register of physiologic races of *Puccinia recondita* f. sp. *tritici*. *Plant Disease Reporter* 50: 756–760.

Kiani T., Mehboob F., Hyder M.Z., Zainy Z., Xu L., … Farrakh S., 2021. Control of stripe rust of wheat using indigenous endophytic bacteria at seedling and adult plant stage. *Scientific Reports* 11: 14473. https://doi.org/10.1038/s41598-021-93939-6.

Kolaei E.A., Cenatus C., Tweddell R.J., Avis T.J., 2013. Antifungal activity of aluminium-containing salts against the development of carrot cavity spot and potato dry rot. *Annals of Applied Biology* 163: 311–317. https://doi.org/10.1111/aab.12056.

Li S., Wang Z., Tang B., Zheng L., Chen H., … Liu D., 2020. A Pathogenesis-Related Protein-Like Gene Is Involved in the Panax notoginseng Defense Response to the Root Rot Pathogen. *Frontiers in Plant Science* 11: 610176.

Liu J., Zong Y., Qin G., Li B., Tian S., 2010. Plasma membrane damage contributes to antifungal activity of silicon against penicillium digitatum. *Current Microbiology* 61: 274–279. https://doi.org/10.1007/s00284-010-9607-4.

Livak K.J., Schmittgen T.D., 2001. Analysis of relative gene expression data using real-time quantitative PCR and the 2-ΔΔCT method. *Methods* 25: 402–408. https://doi.org/10.1006/meth.2001.1262.

Malik C. P. and Singh M. B., 1980. Estimation of total phenols. In: *Plant Enzymology and Histo-Enzymology*. Kalyani Publishers, New Delhi.

Maxwell D.P., Bateman D.F., 1967. Changes in the activities of some oxidases in extracts of Rhizoctonia-infected bean hypocotyls in relation to lesion maturation. *Phytopathology* 57: 132–136.

Merino D., Tomadoni B., Salcedo M.F., Mansilla A.Y., Casalongué C.A., Alvarez V.A., 2021. Nanoclay as Carriers of Bioactive Molecules Applied to Agriculture. In: *Handbook of Nanomaterials and Nanocomposites for Energy and Environmental Applications: Volumes 1-4* (O.V. Kharissova, L.M. Torres-Martínez and B.I. Kharisov, ed.), Cham, Springer International Publishing, 433–454.

Nazir M.S., Mohamad Kassim M.H., Mohapatra L., Gilani M.A., Raza M.R., Majeed K., 2016. Characteristic Properties of Nanoclays and Characterization of Nanoparticulates and Nanocomposites. In: *Engineering Materials* (M. Jawaid, A. el K. Qaiss and R. Bouhfid, ed.), Singapore, Springer Singapore, 35–55.

Oliveira-Pinto P.R., Mariz-Ponte N., Gil R.L., Cunha E., Amorim C.G., … Santos C., 2022. Montmorillonite Nanoclay and Formulation with *Satureja montana* Essential Oil as a Tool to Alleviate Xanthomonas euvesicatoria Load on *Solanum lycopersicum*. *Applied Nano* 126–142.

Peterson R.F., Campbell A.B., Hannah A.E., 1948. A diagrammatic scale for estimating rust intensity on leaves and stems of cereals. *Canadian Journal of Research* 26c: 496–500. https://doi.org/10.1139/cjr48c-033.

Poria V., Rana A., Kumari A., Grewal J., Pranaw K., Singh S., 2021. Current perspectives on chitinolytic enzymes and their agro-industrial applications. *Biology* 10(12):1319. https://doi.org/10.3390/biology10121319.

Rashad Y.M., Aseel D.G., Hafez E.E., 2018. Antifungal potential and defense gene induction in maize against Rhizoctonia root rot by seed extract of Ammi visnaga (L.) Lam. *Phytopathologia Mediterranea* 57: 73–88. https://doi.org/10.14601/Phytopathol_Mediterr-21366.

Rashad Y., Aseel D., Hammad S., 2020a. Phenolic Compounds Against Fungal and Viral Plant Diseases. In: *Plant Phenolics in Sustainable Agriculture* (R. Lone, R. Shuab and A.N. Kamili, ed.), Singapore, Springer Singapore, 201–219.

Rashad Y.M., Abbas M.A., Soliman H.M., Abdel-Fattah G.G., Abdel-Fattah G.M., 2020b. Synergy between endophytic Bacillus amyloliquefaciens GGA and arbuscular mycorrhizal fungi induces plant defense responses against white rot of garlic and improves host plant growth. *Phytopathologia Mediterranea* 59: 169–186. https://doi.org/10.14601/Phyto-11019.

Rashad Y.M., El-Sharkawy H.H.A., Belal B.E.A., Abdel Razik E.S., Galilah D.A., 2021a. Silica Nanoparticles as a Probable Anti-Oomycete Compound Against Downy Mildew, and Yield and Quality Enhancer in Grapevines: Field Evaluation, Molecular, Physiological, Ultrastructural, and Toxicity Investigations. *Frontiers in Plant Science* 12: 763365.

Rashad Y.M., Fekry W.M.E., Sleem M.M., Elazab N.T., 2021b. Effects of Mycorrhizal Colonization on Transcriptional Expression of the Responsive Factor JERF3 and Stress-Responsive Genes in Banana Plantlets in Response to Combined Biotic and Abiotic Stresses. *Frontiers in Plant Science* 12: 742628.

Rashad, Y.M., El-Sharkawy, H.A., Abdalla, S.A., Ibrahim, O. M. and Elazab N.T., 2024. Unraveling the regulation effect of the endophyte Epicoccum nigrum HE20 on the polyphenol biosynthetic pathways genes in wheat against stripe rust. *BMC Plant Biology* 24:

Soltan Y.A., Morsy A.S., Hashem N.M., Elazab M.A.I., Sultan M.A., … Sallam S.M.A., 2022. Potential of montmorillonite modified by an organosulfur surfactant for reducing aflatoxin B1 toxicity and ruminal methanogenesis *in vitro*. *BMC Veterinary Research* 18: 387. https://doi.org/10.1186/s12917-022-03476-1.

Sundaresha S., Sharma S., Bairwa A., Tomar M., Kumar R., … Chakrabarti S.K., 2022. Spraying of dsRNA molecules derived from Phytophthora infestans, along with nanoclay carriers as a proof of concept for developing novel protection strategy for potato late blight. *Pest Management Science* 78: 3183–3192. https://doi.org/10.1002/ps.6949.

Vidossich P., Alfonso-Prieto M., Rovira C., 2012. Catalases versus peroxidases: DFT investigation of H2O 2 oxidation in models systems and implications for heme protein engineering. *Journal of Inorganic Biochemistry* 117: 292–297. https://doi.org/10.1016/j.jinorgbio.2012.07.002.

Wang X., Che M.Z., Khalil H.B., McCallum B.D., Bakkeren G., … Saville B.J., 2020. The role of reactive oxygen species in the virulence of wheat leaf rust fungus *Puccinia triticina*. *Environmental Microbiology* 22: 2956–2967. https://doi.org/10.1111/1462-2920.15063.

Worrall E.A., Hamid A., Mody K.T., Mitter N., Pappu H.R., 2018. Nanotechnology for plant disease management. *Agronomy* 8(12): 285.

Yousef H.A., Fahmy H.M., Arafa F.N., Abd Allah M.Y., Tawfik Y.M., … Bassily M.E., 2023. Nanotechnology in pest management: advantages, applications, and challenges. *International Journal of Tropical Insect Science* 43: 1387–1399. https://doi.org/10.1007/s42690-023-01053-z.

Zhang H., Liu W., Wan L., Li F., Dai L., … Huang R., 2010. Functional analyses of ethylene response factor JERF3 with the aim of improving tolerance to drought and osmotic stress in transgenic rice. *Transgenic Research* 19: 809–818. https://doi.org/10.1007/s11248-009-9357-x.

Zhang S., 2023. Recent Advances of Polyphenol Oxidases in Plants. *Molecules* 28(5): 2158.

Zhao J., Zhang H., Yao J., Paul S., 2011. Identifcation of Berberis spp. as alternate hosts of *Puccinia striiformis* f. sp. *tritici* in China. *Borlaug Global Rust Initiative workshop*, *Mycosystema* 30: 167.